Published in final edited form as:
Neuropharmacology. 2014 April ; 79: 542–549. doi:10.1016/j.neuropharm.2014.01.005.

Probing NMDA receptor GluN2A and GluN2B subunit expression and distribution in cortical neurons

Rashna D. Balsara[a], **Ashley N. Ferreira**[b], **Deborah L. Donahue**[a], **Francis J. Castellino**[a,c], and **Patrick L. Sheets**[b,d]

[a]W.M. Keck Center for Transgene Research, University of Notre Dame, Notre Dame, IN, USA

[b]Department of Biological Sciences, University of Notre Dame, Notre Dame, IN, USA

[c]Department of Chemistry and Biochemistry, University of Notre Dame, Notre Dame, IN, USA

[d]Department of Pharmacology and Toxicology, Indiana University School of Medicine-South Bend, South Bend, IN, USA

Abstract

The spatial distribution of N-methyl-D-aspartate receptor (NMDAR) subunits in layer 5 (L5) neurons of the medial prefrontal cortex (mPFC) is important for integrating input-output signals involved in cognitive functions and motor behavior. In this study, focal laser scanning photostimulation of caged glutamate, slice electrophysiology, and small peptide pharmacology, were used to map the distribution of functional GluN2A and GluN2B subunits of the NMDAR from L5 neurons of wild-type (WT) and GluN2A$^{-/-}$ mice. Focal uncaging of glutamate evoked spatially-restricted glutamatergic responses on various dendritic locations of pyramidal neurons in the mPFC. Analyses of the spatial arrangements of the GluN2A and GluN2B subunits were performed by comparing inhibition of glutamatergic responses in the presence of the GluN2A-selective pharmacological antagonist, NVP-AAM077 (NVP), and the GluN2B-selective peptidic antagonist, conantokin-G (con-G). We found that apical and basal expression and distribution of GluN2A and GluN2B were similar in L5 mPFC neurons of WT mice. However, the inhibition of glutamatergic responses by NVP in brain slices of GluN2A$^{-/-}$ mice were dramatically decreased, while con-G inhibition remained similar to that observed in WT brain slices. The data obtained show that expression and spatial arrangement of GluN2B subunits is independent of GluN2A in L5 neurons of the mPFC. These findings have important ramifications for NMDAR organization and function in L5 pyramidal neurons of the mPFC, and show that specific populations of NMDARs can be antagonized, while sparing other subgroups of NMDARs, thus preserving selective NMDAR functions, an important therapeutic advantage.

Correspondence: Patrick L. Sheets, Indiana University School of Medicine-South Bend, 127 Raclin-Carmichael Hall, 1234 Notre Dame Ave, South Bend, IN 46617, plsheets@iupui.edu; telephone: 574-631-7193, or Francis J. Castellino, W.M. Keck Center for Transgene Research, 230 Raclin-Carmichael Hall, University of Notre Dame, Notre Dame, IN, USA 46556, fcastell@nd.edu; telephone: 574-631-8996.

RDB and ANF contributed equally to the experimental portions of this work.

Author contributions

ANF, RDB, and PLS performed all experiments and analysis, with contributions from DLD. FJC, RDB, and PLS wrote the paper.

Keywords

NMDARs; pyramidal L5 neurons; conantokins; slice electrophysiology; medial prefrontal cortex; laser-scanning photostimulation

1. Introduction

N-methyl-D-aspartate receptors (NMDARs) expressed at excitatory synapses are coactivated by glutamate and glycine, and are critical for the Ca^{2+}-dependent plasticity that facilitates learning and memory, as well as for interneuron communication. In addition, the NMDAR is also involved in different neuropathologies (Bliss and Collingridge, 1993; Waxman and Lynch, 2005). Although NMDARs are ubiquitously expressed in the central nervous system, their exact subunit compositions, and spatial and temporal distributions in the cortex, may reflect the specialized functions of local circuits. NMDARs are heterotetrameric combinations of two mandatory GluN1 subunits (a-h splice variants of a single GluN1 gene) and two GluN2 (A-D of separate GluN2 genes) subunits. The GluN2 subunit confers distinct biochemical properties on the NMDAR, which affect the intrinsic behavior and downstream signaling pathways of this receptor. GluN2B-rich synapses in the prefrontal cortex circuitry are pivotal for online processing due to generation of slow recurrent dynamics that form an integral part of working memory and decision-making (Wang et al., 2008). Conversely, the visual cortex is rich in GluN2A-containing synapses, resulting in shorter NMDA currents, and is essential for modulation of experience-dependent synaptic plasticity (Quinlan et al., 1999).

Compromised NMDAR signaling accompanied by preferential changes in subunit composition is observed in various neuropathologies. Restricted expression of the GluN1/GluN2B receptor has been discovered in areas involved in pain signaling, such as dorsal root ganglion, spinal dorsal horn, and cortex (Buller et al., 1994; Kim et al., 2012; Millecamps et al., 2007). Pathological pain causes increased GluN2B expression in the prefrontal cortex, which is thought to alter the emotional integration of nociception (Wei et al., 2001). Increased GluN2B expression has been observed in the spinal cord following nerve injury (Kim et al., 2012). Conversely, occlusion of the middle carotid artery decreased the levels of GluN2A and GluN2B in the ischemic core of stroked rats (Picconi et al., 2006). Therefore, detecting changes in the molecular heterogeneity of NMDAR distribution and expression in cortical neurons, specifically of the GluN2A and GluN2B subunits, will provide insight into the pathology of various neurological disorders.

Conantokin-G (con-G), a small polypeptide present in the venom of the cone-snail, *Conus geographus*, is a selective antagonist that acts on the GluN2B subunit of NMDARs (Sheng et al., 2009). The GluN2B-specificity of con-G makes it an attractive candidate for remedying NMDAR-driven neuropathologies, many of which rely on GluN2B for their pathogenic properties. In this study, we utilized the GluN2B-specificity of con-G to elucidate GluN2B distribution in L5 pyramidal neurons in the mPFC. Collectively, these neurons are pivotal in integrating and eliciting descending commands that affect a multitude of physiological responses including fear and addiction (Peters et al., 2009) and learning and memory (Euston et al., 2012).. However, the effects of alterations in GluN2B expression and distribution within mPFC neurons that are involved in descending pain circuits and specific neuropathologies, such as stroke, are not known.

Our goal was to test the feasibility of mapping NMDA-GluN2 subunit expression using the pharmacology of GluN2B-selective antagonist, con-G, and NVP-AAM077 (NVP), a weak GluN2A-selective antagonist at low concentrations, in combination with focal glutamate

uncaging via laser scanning photostimulation (glu-LSPS). Combining these methods, we were able to produce a relatively rapid and efficient assessment of the NMDAR subunit distribution in cortical neurons. In this study, we show that L5 neurons of mPFC have similar GluN2A and GluN2B expression and distribution, a finding of high relevance to the potential of selective inhibition of a population or receptors in brain.

2. Materials and Methods

2.1. Con-G synthesis

Solid phase peptide synthesis (Applied Biosystems, Model 433A) was employed to chemically synthesize con-G ($GE\gamma\gamma L^{5}Q\gamma NQ\gamma^{10}LIR\gamma K^{15}SN\text{-}NH_2$; γ= gamma-carboxyglutamate) according to methods published earlier (Prorok et al., 1996).

2.2. Mice

Postnatal day 21–33, WT mice (C57Bl/6J; Jackson Laboratories, Bar Harbor, ME) and $GluN2A^{-/-}$ mice (Sakimura et al., 1995), obtained from Gary Westbrook, Oregon Health and Science University, of either gender were used for these studies. Animal studies were conducted in accordance with the animal care and use guidelines of Indiana University, University of Notre Dame, National Institutes of Health, and the Society for Neuroscience.

2.3. Brain slice preparation

Brain slices were prepared as described (Sheets et al., 2011). Coronal slices (coronal slice angle tilted rostrally 10–15 degrees; 300 μm thick) containing the medial prefrontal cortex (mPFC) were made by vibratome-sectioning the brain (VT1200S, Leica) in chilled cutting solution (composed of: 110 mM choline chloride, 25 mM $NaHCO_3$, 25 mM D-glucose, 11.6 mM sodium ascorbate, 7 mM $MgSO_4$, 3.1 mM sodium pyruvate, 2.5 mM KCl, 1.25 mM NaH_2PO_4, and 0.5 mM $CaCl_2$). Slices were transferred to artificial cerebrospinal fluid (ACSF, composed of: 127 mM NaCl, 25 mM $NaHCO_3$, 25 mM D-glucose, 2.5 mM KCl, 1 mM $MgCl_2$, 2 mM $CaCl_2$, and 1.25 mM NaH_2PO_4, aerated with 95% O_2 /5% CO_2) at 35–37° C for 30 min. Slices were subsequently incubated in ACSF at 22° C for at least 1 hr prior to electrophysiological recordings.

2.4. Electrophysiology

Whole cell, patch-clamp recordings were obtained with glass pipettes filled with intracellular solution composed of: 128 mM K-gluconate, 10 mM HEPES, 1 mM EGTA, 4 mM $MgCl_2$, 4 mM ATP, 0.4 mM GTP, 10 mM phosphocreatine, 3 mM ascorbate, and 0.05 mM Alexa-594 hydrazide (Life Technologies/Molecular Probes, Grand Island, NY), pH 7.3. Recordings were filtered at 4 KHz and sampled at 10 KHz. Neurons were visualized using video-enhanced infrared gradient contrast optics (Dodt and Zieglgansberger, 1994) and recorded at 22° C.

2.5. Direct mapping using glutamate uncaging and laser scanning photostimulation

Glutamate uncaging and laser scanning photostimulation (glu-LSPS) were performed as described previously (Sheets et al., 2011), using an ultraviolet laser (355 nm; RPMC Lasers, O'Fallon, MO). Stock solutions of MNI-caged glutamate (50 mM in water; Tocris/R&D Systems, Minneapolis, MN) were prepared at room temperature to avoid precipitation, sonicated, aliquoted, and stored at −20°C until use. *Ephus* software (http://www.ephus.org) was used for hardware control and data acquisition (Suter et al., 2010). Before dendritic mapping studies were initiated, a low magnification image of the slice was acquired. The mapping area grid was 8 × 16 with 50 μm spacing which gives an uncaging area of approximately 320,000 um^2 and 128 uncaging sites. Caged glutamate (0.2 mM; MNI-

glutamate, Tocris) was added to the bath solution. (4*R*,4a*R*,5*R*,6*S*,7*S*,8*S*,8a*R*,10*S*,12*S*)-2-azaniumylidene-4,6,8,12-tetrahydroxy-6-(hydroxymethyl)-2,3,4,4a,5,6,7,8-octahydro-1*H*-8a,10-methano-5,7-(epoxymethanooxy)quinazolin-10-olate (TTX; 0.5 μM) was added to eliminate inputs from presynaptic neurons and 4-ethylphenylamino-1,2-dimethyl-6-methylaminopyrimidinium chloride (ZD 7288; 25 μM) was added to eliminate dendritic filtering due to hyperpolarization-activated current). The power of the UV laser was set to 20 mW in the specimen plane. During mapping, stimulus sites were visited at 0.67 Hz in a non-raster pattern that avoided the vicinity of recently stimulated sites (Shepherd et al., 2003). Excitatory responses were acquired at the level of the soma following glutamatergic stimulation at the various 128 locations across the uncaging area. Responses were recorded in the current-clamp mode, and analyzed off-line to determine the mean depolarization over a 0.75 sec post-stimulus window. Direct mapping was performed, before and after addition of con-G (2 μM) or NVP (100 nM; a gift from Y.P. Auberson, Novartis, Basel, Switzerland).

2.6. Two-photon imaging

Two-photon imaging was performed on an Olympus FV1000 multiphoton microscope. Images were acquired using an Olympus 25× water objective at 1024 × 1024 pixel resolution at a rate of 4 msec/pixel. Traces were stitched and converted to the .tiff format using Neurolucida software (MBF Bioscience, Williston, VT).

2.7. Statistical analysis

Data analysis was performed offline using Matlab routines (Mathworks, Natick, MA). Group comparisons were tested using a paired Student's *t*-test. Error bars in plots represent the standard error of the mean (S.E.M.).

3. Results

After preparing brain slices, pyramidal neurons (readily observed) were targeted for electrophysiological recording in L5 of the mPFC, which is the major output layer of the cortex. To test the effects of con-G (2 μM) on glutamatergic responses, we recorded from the *soma* of neurons, in the presence of 0.5 μM TTX, to block presynaptic inputs, and 25 μM ZD 7288, to dampen dendritic filtering. Responses were evoked at an array of locations across their dendritic arbors using focal glutamate uncaging (Figure 1A), before and after con-G application. Con-G-sensitive components were determined by subtracting treated traces from control traces (Figure 1B). Somatic responses were arranged as a trace map (8 × 16, 50 μm spacing) showing locations of dendritic stimulation (Figure 1C). Trace maps were then converted to representative color maps (Figure 1D).

On average, con-G significantly decreased glutamatergic responses, suggesting strong GluN2B expression in NMDARs of L5 mPFC neurons (Figure 2A). The vertical profiles of average responses (Figure 2B) showed dramatic con-G effects across all dendritic locations. When dividing the mapping grid into regions of interest that focused on apical and basal dendritic locations (Figure 2C), we found that con-G showed similar blocking effects in both regions (Figure 2D; Table 1). This indicated a broad and similar distribution of GluN2B in NMDARs at the apical, basal, and dendritic locations.

For comparison, the effects of NVP were examined, which at low concentrations (100 nM), is a weak competitive antagonist for the NMDAR subunit GluN2A (Auberson et al., 2002). Similar to con-G, NVP also decreased glutmatergic responses at all dendritic locations (Figure 2E, F). Significant decreases, while not as dramatic as con-G effects, were observed at both apical and dendritic locations (Figure 2G, H; Table 1). Comparison of the mean NVP

and con-G-sensitive traces in the WT brain slices showed dramatically different kinetics (Figure 3A, B), suggesting that the observed decreases for the two groups were the result of blocking two different types of glutamatergic current. Overall, the results from these experiments suggest that GluN2A expression and distribution is similar to GluN2B in NMDAR receptors in L5 mPFC neurons.

To confirm that our methodology was effectively showing NMDAR subunit responses, the effects of NVP and con-G in brain slices of GluN2A$^{-/-}$ mice were examined. Our hypothesis was that low concentrations of NVP would show little or no effect on responses elicited by glutamate uncaging in GluN2A$^{-/-}$ slices, while inhibition by con-G would be unaffected from that seen in WT neurons. The morphological appearance of L5 mPFC neurons in GluN2A$^{-/-}$ mice was similar to WT neurons (Figure 4A). There were no significant differences in the magnitude of dendritic responses to caged glutamate between WT and GluN2A$^{-/-}$ neurons (Figure 4B, C). The average radial profile appears different between WT and GluN2A$^{-/-}$ neurons (Figure 4C). This is likely due to the *somata* from the GluN2A$^{-/-}$ data set being slightly closer to the *pia* than in WT slices. Glutamatergic potentials recorded from apical and basal areas of GluN2A$^{-/-}$ mice showed slower activation and decay when compared to WT potentials (Figure 4D). On average, con-G-sensitive traces in GluN2A$^{-/-}$ neurons displayed a slightly slower decay than WT neurons. One possibility for this difference is that con-G inhibited a mixture of GluN1/Glu2A/Glu2B triheteromeric receptors in WT-neurons, while blocking GluN1/GluN2B receptors in GluN2A$^{-/-}$ neurons.

We found that NVP had a significantly reduced inhibitory effect on glutamatergic responses (Figure 5A, B) in GluN2A$^{-/-}$ neurons for both apical and basal dendritic locations, when compared to WT neurons (Figure 5C, D; Table 1). However, a small but significant decrease in basal dendritic responses following NVP treatment was observed. The difference is a result of 1 out 6 recorded neurons showing a dramatic decrease in glutamatergic response, suggesting some unsurprising variability in the NVP pharmacology. The comparison of NVP-sensitive traces between WT and GluN2A$^{-/-}$ mice showed different onset and decay (Figure 6A, B), suggesting that NVP, even at 100 nM, may be competitively inhibiting a small percentage of other NMDAR subunits, such as GluN2B, GluN2C, and/or GluN2D. This limitation of NVP has been previously reported (Frizelle et al., 2006; Neyton and Paoletti, 2006). Yet, we did observe a dramatically decreased NVP effect in GluN2A$^{-/-}$ neurons suggesting that 100 nM NVP primarily antagonized GluN2A subunits. Conversely, con-G inhibition was preserved, significantly reducing glutamatergic responses, for L5 mPFC neurons at both apical and basal dendritic locations (Figure 5E-H). Con-G sensitive traces showed similar onset kinetics but had subtle differences in decay (Figure 6C, D), which could be due to the absence of GluN1/Glu2A/Glu2B triheteromeric receptors in GluN2A$^{-/-}$ mice. Taken together, these results indicated that levels and spatial arrangement of GluN2B-containing NMDAR channels were maintained in the absence of GluN2A subunits.

4. Discussion

NMDARs are of ongoing interest in many fields of neurobiology such as learning and memory, neurological disorders, and brain injury. Assessment of changes in expression, distribution, and function of NMDARs is, therefore, critical. Here, we exploited the pharmacology of GluN2B antagonist, con-G, and GluN2A competitive antagonist, NVP, to probe expression and distribution of NMDAR subunits in neurons in the mPFC using glutamate uncaging *via* laser scanning photostimulation. This method allowed analysis of not only the magnitude of con-G and NVP effects, but also the relative distribution of such effects. Con-G and NVP inhibitions of excitatory potentials induced by glutamate uncaging

were not significantly different from each other, suggesting similar expression and distribution of GluN2A and GluN2B subunits in L5 pyramidal mPFC neurons. However, it is noted that glu-LSPS mapping represents responses elicited from both synaptic and extrasynaptic sites. It was originally thought that in the adult CNS, the synapses are rich in GluN2A subunits, while the extrasynaptic sites are enriched with GluN2B subunits (Liu et al., 2007). However recent findings demonstrated that GluN2A is a minor synaptic component and that GluN2B plays a dichotomous role in synaptic- and extrasynaptic-potentiation (Martel et al., 2009). Our mapping data demonstrated that GluN2A and GluN2B levels were similar, which is in agreement with published data showing that GluN2A and GluN2B levels remain unchanged in the PFC of both young and adult rats (Wang et al., 2008). Traces displaying con-G sensitive components of the glutamatergic responses displayed much slower onset and decay than NVP sensitive components, thus showing that con-G and NVP were inhibiting different NMDA-GluN subunits, irrespective of their synaptic or extrasynaptic locations. It has been demonstrated that layer 5 of the prefrontal cortex express similar levels of GluN2A and GluN2B, low levels of GluN2C, and intermediate levels of GluN2D (Akbarian et al., 1996), thus indicating that neuronal synaptic inputs and integration is governed by heterogeneity of different NMDAR subunits by conferring different gating behaviors, responses to Mg^{2+}, and current/voltage activity. From published data it has been demonstrated that specific inhibition of either GluN2A or GluN2B did not affect synaptic inputs mediated by GluN2C or GluN2D (Kumar and Huguenard et al., 2003).

Although there was a significant reduction in NVP-mediated inhibition of glutamatergic responses for neurons from GluN2A$^{-/-}$ mice, the con-G inhibitory effect remained unchanged. This implies that there was no significant change in the expression or distribution of GluN2B subunits in the GluN2A$^{-/-}$ mice and that the GluN2A subunit is not essential for NMDAR-dependent synaptic activation. Our observations reflect previously published data which demonstrated that NR2A deficiency did not affect expression levels of NR2B in the visual cortex (Philpot et al., 2007), or in the somatosensory cortex (Abdrachmanova et al., 2001), and that long term potentiation in the bed nucleus of the *stria terminalis* slices was not compromised in the GluN2A$^{-/-}$ brains, compared to WT brains (Weitlauf et al., 2005). Whereas expression of the mandatory GluN1 subunit is widespread in the brain, the different splice variants (GluN1a-h) have distinct spatial and temporal expression patterns. The various splice variant combinations of GluN1a-h with either GluN2A or GluN2B imparts different electrophysiological and pharmacokinetic properties, and thereby contribute towards region-specific functional heterogeneity (Laurie et al., 1995).

Alteration of specific NMDAR subunits is becoming increasingly critical for assessing a variety of neuronal mechanisms such as synaptic plasticity (Cull-Candy et al., 2001; Paoletti et al., 2013). The ratios, expression, and activity of NMDAR subunits are significant in memory function (Brim et al., 2013; Clayton et al., 2002) and the underlying pathology of pain (Boyce et al., 1999; Xiao et al., 2008), depression (Autry et al., 2011), brain injury (Aarts et al., 2002), and cognitive and motor neuropathologies (Gardoni et al., 2012; Mota et al., 2013; Piyabhan et al., 2013; Vastagh et al., 2012). Recent publications have discerned the direct effect of conantokin/receptor interaction on neuronal cell signaling and pathophysiological responses (Balsara et al., 2012; Huang et al., 2010). It has been well established that con-G is a specific antagonist of the NR2B subunit (Alex et al., 2006; Donevan and McCabe, 2000; Klein et al., 2001). The GluN2B-specificity of con-G makes it an attractive candidate for probing GluN2B expression and for potentially remedying GluN2B-driven neuropathologies. Previous studies have demonstrated that con-G, and another related conotoxins, have anti-nociceptive properties, however psycho-mimetic side-effects persisted (Hama and Sagen, 2009; Xiao et al., 2008). In addition, con-G has shown therapeutic potential for brain injury (Williams et al., 2003), opioid withdrawal (Wei et al.,

2006), and epilepsy (Barton et al., 2004). NMDAR subunit expression, in particular the GluN2B subunit, changes in the frontal/prefrontal cortex as the mice age. It has also been reported (Ontl et al., 2004) that GluN1 expression did not change significantly with aging, but expression of the GluN2B subunit was highest in 13–15 day old mice, then starts to diminish at 49–53 days, after which it plateaus at that level as the mice age to 25 months. This also corresponded to a decline in binding to glutamate. A similar developmental-dependent expression pattern of GluN2B was observed in the cortex of rats, where it is highest at P12–30 and then declines with maturity (Kew et al., 1998; Sheng et al., 1994). There is very little expression of the GluN2A subunit at P0, but it increases around postnatal week 3 and is expressed uniformly throughout the brain. This increase in GluN2A is associated with experience-dependent plasticity, and roughly corresponds to the developmental decrease of GluN2B expression levels (Geddes et al., 2011). Since the prefrontal cortex is associated with neuropsychiatric disorders, such as schizophrenia, functional mapping of the GluN subunits in a regio-specific and developmental manner may further our understanding as to how these receptors regulate various neuropathophysiologies.

This study shows that neurons across cortical layers and regions could be probed for NMDAR subunit ‘hot spots’, which are of great value in focal excitation and signaling. Mapping of the GluN2B subunit expression throughout the dendritic area of cortical neurons is quite informative, as the extent of Con-G inhibition was much more dramatic perisomatically, but still significant in apical areas. This distribution of GluN2B is of importance in long-range and local integration of excitatory synaptic inputs. It is known from electro-anatomical studies of the mouse motor cortex that strong excitatory projections from layer 2/3 to layer 5A/B occur (Hooks et al., 2013; Weiler et al., 2008). Further, microcircuit targeting is determined by both laminar location and projection target of the post-synaptic soma (Anderson et al., 2010). Using con-G, expression and distribution of GluN2B could be determined in retrogradely-labeled neurons near the L5A/B border in the motor cortex. We hypothesize that the strongest con-G effect would be at basal dendrites contained within the L5A/B border. Established local circuit pathways in other cortical areas, such as somatosensory (Shepherd et al., 2005; Shepherd and Svoboda, 2005), and auditory (Oviedo et al., 2010), could be analyzed in a similar manner. Theoretically, dendrites receiving the strongest local input should have the greatest NMDAR expression. Questions remain as to what NMDAR subunits are involved in these local circuits. In addition, effects of con-G on long-range inputs to cortex could be evaluated using optogenetics (Hooks et al., 2013; Petreanu et al., 2007), and could potentially reveal differences in the role of NMDARs in processing long *versus* local excitatory input in the cortex.

Acknowledgments

Support: This work was supported by grant HL019982 from the N.I.H. (to F.J.C.)

We thank the Flow Cytometry and Imaging Core at Indiana University School of Medicine for use of the Olympus multiphoton imaging microscope. We also thank Sarah Dalton for contributions to the two-photon imaging.

References

Aarts M, Liu Y, Liu L, Besshoh S, Arundine M, Gurd JW, Wang YT, Salter MW, Tymianski M. Treatment of ischemic brain damage by perturbing NMDA receptor-PSD-95 protein interactions. Science. 2002; 298:846–850. [PubMed: 12399596]

Abdrachmanova G, Chodounska H, Vyklicky L. Effects of steroids on NMDA receptors and excitatory synaptic transmission in neonatal motoneurons in rat spinal cord slices. Eur J Neurosci. 2001; 14:495–502. [PubMed: 11553299]

Akbarian S, Sucher NJ, Bradley D, Tafazzoli A, Trinh D, Hetrick WP, Potkin SG, Sandman CA, Bunney WE Jr, Jones EG. Selective alterations in gene expression of NMDA receptor subunits in prefrontal cortex of schizophrenics. J Neurosci. 1996; 16:19–30. [PubMed: 8613785]

Alex AB, Baucum AJ, Wilcox KS. Effect of Conantokin G on NMDA receptor-mediated spontaneous EPSCs in cultured cortical neurons. J Neurophysiol. 2006; 96:1084–1092. [PubMed: 16760339]

Anderson CT, Sheets PL, Kiritani T, Shepherd GM. Sublayer-specific microcircuits of corticospinal and corticostriatal neurons in motor cortex. Nat Neurosci. 2010; 13:739–744. [PubMed: 20436481]

Auberson YP, Allgeier H, Bischoff S, Lingenhoehl K, Moretti R, Schmutz M. 5-phosphonomethylquinoxalinediones as competitive NMDA receptor antagonists with a preference for the human 1A/2A, rather than 1A/2B receptor composition. Bioorg Med Chem Lett. 2002; 12:1099–1102. [PubMed: 11909726]

Autry AE, Adachi M, Nosyreva E, Na ES, Los MF, Cheng PF, Kavalali ET, Monteggia LM. NMDA receptor blockade at rest triggers rapid behavioural antidepressant responses. Nature. 2011; 475:91–95. [PubMed: 21677641]

Balsara R, Li N, Weber-Adrian D, Huang L, Castellino FJ. Opposing action of conantokin-G on synaptically and extrasynaptically-activated NMDA receptors. Neuropharmacology. 2012; 62:2227–2238. [PubMed: 22306487]

Barton ME, White HS, Wilcox KS. The effect of CGX-1007 and CI-1041, novel NMDA receptor antagonists, on NMDA receptor-mediated EPSCs. Epilepsy Res. 2004; 59:13–24. [PubMed: 15135163]

Bliss TV, Collingridge GL. A synaptic model of memory: long-term potentiation in the hippocampus. Nature. 1993; 361:31–39. [PubMed: 8421494]

Boyce S, Wyatt A, Webb JK, O'Donnell R, Mason G, Rigby M, Sirinathsinghji D, Hill RG, Rupniak NM. Selective NMDA NR2B antagonists induce antinociception without motor dysfunction: correlation with restricted localisation of NR2B subunit in dorsal horn. Neuropharmacology. 1999; 38:611–613. [PubMed: 10340299]

Brim BL, Haskell R, Awedikian R, Ellinwood NM, Jin L, Kumar A, Foster TC, Magnusson KR. Memory in aged mice is rescued by enhanced expression of the GluN2B subunit of the NMDA receptor. Behav Brain Res. 2013; 238:211–226. [PubMed: 23103326]

Buller AL, Larson HC, Schneider BE, Beaton JA, Morrisett RA, Monaghan DT. The molecular basis of NMDA receptor subtypes: native receptor diversity is predicted by subunit composition. J Neurosci. 1994; 14:5471–5484. [PubMed: 7916045]

Clayton DA, Grosshans DR, Browning MD. Aging and surface expression of hippocampal NMDA receptors. J Biol Chem. 2002; 277:14367–14369. [PubMed: 11891215]

Cull-Candy S, Brickley S, Farrant M. NMDA receptor subunits: diversity, development and disease. Curr Opin Neurobiol. 2001; 11:327–335. [PubMed: 11399431]

Dodt HU, Zieglgansberger W. Infrared videomicroscopy: a new look at neuronal structure and function. Trends Neurosci. 1994; 17:453–458. [PubMed: 7531885]

Donevan SD, McCabe RT. Conantokin G is an NR2B-selective competitive antagonist of N-methyl-D-aspartate receptors. Mol Pharmacol. 2000; 58:614–623. [PubMed: 10953056]

Euston DR, Gruber AJ, McNaughton BL. The role of medial prefrontal cortex in memory and decision making. Neuron. 2012; 76:1057–1070. [PubMed: 23259943]

Frizelle PA, Chen PE, Wyllie DJ. Equilibrium constants for (R)-[(S)-1-(4-bromo-phenyl)-ethylamino]-(2,3-dioxo-1,2,3,4-tetrahydroquinoxalin-5-yl)-methyl]-phosphonic acid (NVP-AAM077) acting at recombinant NR1/NR2A and NR1/NR2B N-methyl-D-aspartate receptors: Implications for studies of synaptic transmission. Mol Pharmacol. 2006; 70:1022–1032. [PubMed: 16778008]

Gardoni F, Sgobio C, Pendolino V, Calabresi P, Di Luca M, Picconi B. Targeting NR2A-containing NMDA receptors reduces L-DOPA-induced dyskinesias. Neurobiol Aging. 2012; 33:2138–2144. [PubMed: 21821315]

Geddes AE, Huang XF, Newell KA. Reciprocal signalling between NR2 subunits of the NMDA receptor and neuregulin1 and their role in schizophrenia. Prog Neuro-Psychopharm Biol Psychiatry. 2011; 35:896–904.

Hama A, Sagen J. Antinociceptive effects of the marine snail peptides conantokin-G and conotoxin MVIIA alone and in combination in rat models of pain. Neuropharmacology. 2009; 56:556–563. [PubMed: 19010337]

Hooks BM, Mao T, Gutnisky DA, Yamawaki N, Svoboda K, Shepherd GM. Organization of cortical and thalamic input to pyramidal neurons in mouse motor cortex. J Neurosci. 2013; 33:748–760. [PubMed: 23303952]

Huang L, Balsara RD, Sheng Z, Castellino FJ. Conantokins inhibit NMDAR-dependent calcium influx in developing rat hippocampal neurons in primary culture with resulting effects on CREB phosphorylation. Mol Cell Neurosci. 2010; 45:163–172. [PubMed: 20600930]

Kew JNC, Richards JG, Mutel V, Kemp JA. Developmental changes in NMDA receptor glycine affinity and ifenprodil sensitivity reveal three distinct populations of NMDA reeptors in individual rat cortical neurons. J Neurosci. 1998; 18:1935–1943. [PubMed: 9482779]

Kim Y, Cho HY, Ahn YJ, Kim J, Yoon YW. Effect of NMDA NR2B antagonist on neuropathic pain in two spinal cord injury models. Pain. 2012; 153:1022–1029. [PubMed: 22424878]

Klein RC, Prorok M, Galdzicki Z, Castellino FJ. The amino acid residue at sequence position 5 in the conantokin peptides partially governs subunit-selective antagonism of recombinant N-methyl-D-aspartate receptors. J Biol Chem. 2001; 276:26860–26867. [PubMed: 11335724]

Kumar SS, Huguenard JR. Pathway-specific differences in subunit composition of synaptic NMDA receptors on pyramidal neurons in neocortex. J Neurosci. 2003; 31:10074–10083. [PubMed: 14602822]

Laurie DJ, Putzke J, Zieglgansberger W, Seeburg PH, Tolle TR. The distribution of splice variants of the NMDAR1 subunit mRNA in adult rat brain. Brain Res. 1995; 32:94–108.

Liu L, Wang C, Ni X, Sun J. A rapid inhibition of NMDA receptor current by corticosterone in cultured hippocampal neurons. Neurosci Lett. 2007; 420:245–250. [PubMed: 17540506]

Martel MA, Wyllie DJ, Hardingham GE. In developing hippocampal neurons, NR2B-containing N-methyl-D-aspartate receptors (NMDARs) can mediate signaling to neuronal survival and synaptic potentiation, as well as neuronal death. Neuroscience. 2009; 158:334–343. [PubMed: 18378405]

Millecamps M, Centeno MV, Berra HH, Rudick CN, Lavarello S, Tkatch T, Apkarian AV. D-cycloserine reduces neuropathic pain behavior through limbic NMDA-mediated circuitry. Pain. 2007; 132:108–123. [PubMed: 17449176]

Mota SI, Ferreira IL, Rego AC. Dysfunctional synapse in Alzheimer's disease - A focus on NMDA receptors. Neuropharmacology. 201310.1016/j.neuropharm.2013.1008.1013

Neyton J, Paoletti P. Relating NMDA receptor function to receptor subunit composition: limitations of the pharmacological approach. J Neurosci. 2006; 26:1331–1333. [PubMed: 16452656]

Ontl T, Xing L, Bai L, Kennedy E, Nelson S, Wakeman M, Magnusson K. Development and aging of N-methyl-D-asparate receptor expression in the prfrontal/frontal cortex of mice. Neurosci. 2004; 123:467–479.

Oviedo HV, Bureau I, Svoboda K, Zador AM. The functional asymmetry of auditory cortex is reflected in the organization of local cortical circuits. Nat Neurosci. 2010; 13:1413–1420. [PubMed: 20953193]

Paoletti P, Bellone C, Zhou Q. NMDA receptor subunit diversity: impact on receptor properties, synaptic plasticity and disease. Nat Rev Neurosci. 2013; 14:383–400. [PubMed: 23686171]

Peters J, Kalivas PW, Quirk GJ. Extinction circuits for fear and addiction overlap in prefrontal cortex. Learn Mem. 2009; 16:279–288. [PubMed: 19380710]

Petreanu L, Huber D, Sobczyk A, Svoboda K. Channelrhodopsin-2-assisted circuit mapping of long-range callosal projections. Nat Neurosci. 2007; 10:663–668. [PubMed: 17435752]

Philpot BD, Cho KK, Bear MF. Obligatory role of NR2A for metaplasticity in visual cortex. Neuron. 2007; 53:495–502. [PubMed: 17296552]

Picconi B, Tortiglione A, Barone I, Centonze D, Gardoni F, Gubellini P, Bonsi P, Pisani A, Bernardi G, Di Luca M, Calabresi P. NR2B subunit exerts a critical role in postischemic synaptic plasticity. Stroke. 2006; 37:1895–1901. [PubMed: 16741178]

Piyabhan P, Wetchateng T, Sireeratawong S. Cognitive enhancement effects of Bacopa monnieri (Brahmi) on novel object recognition and NMDA receptor immunodensity in the prefrontal cortex

and hippocampus of sub-chronic phencyclidine rat model of schizophrenia. J Med Assoc Thai. 2013; 96:231–238. [PubMed: 23936991]

Prorok M, Warder SE, Blandl T, Castellino FJ. Calcium binding properties of synthetic gamma-carboxyglutamic acid-containing marine cone snail “sleeper” peptides, conantokin-G and conantokin-T. Biochemistry. 1996; 35:16528–16534. [PubMed: 8987986]

Quinlan EM, Philpot BD, Huganir RL, Bear MF. Rapid, experience-dependent expression of synaptic NMDA receptors in visual cortex *in vivo*. Nat Neurosci. 1999; 2:352–357. [PubMed: 10204542]

Sakimura K, Kutsuwada T, Ito I, Manabe T, Takayama C, Kushiya E, Yagi T, Aizawa S, Inoue Y, Sugiyama H, Mishina M. Reduced hippocampal LTP and spatial learning in mice lacking NMDA receptor epsilon 1 subunit. Nature. 1995; 373:151–155. [PubMed: 7816096]

Sheets PL, Suter BA, Kiritani T, Chan CS, Surmeier DJ, Shepherd GM. Corticospinal-specific HCN expression in mouse motor cortex: I(h)-dependent synaptic integration as a candidate microcircuit mechanism involved in motor control. J Neurophysiol. 2011; 106:2216–2231. [PubMed: 21795621]

Sheng M, Cummings J, Roldan LA, Jan YA. Changing subunit composition of heteromeric NMDA receptors during development of rat cortex. Nature. 1994; 368:144–147. [PubMed: 8139656]

Sheng Z, Liang Z, Geiger JH, Prorok M, Castellino FJ. The selectivity of conantokin-G for ion channel inhibition of NR2B subunit-containing NMDA receptors is regulated by amino acid residues in the S2 region of NR2B. Neuropharmacology. 2009; 57:127–136. [PubMed: 19427876]

Shepherd GM, Pologruto TA, Svoboda K. Circuit analysis of experience-dependent plasticity in the developing rat barrel cortex. Neuron. 2003; 38:277–289. [PubMed: 12718861]

Shepherd GM, Stepanyants A, Bureau I, Chklovskii D, Svoboda K. Geometric and functional organization of cortical circuits. Nat Neurosci. 2005; 8:782–790. [PubMed: 15880111]

Shepherd GM, Svoboda K. Laminar and columnar organization of ascending excitatory projections to layer 2/3 pyramidal neurons in rat barrel cortex. J Neurosci. 2005; 25:5670–5679. [PubMed: 15958733]

Suter BA, O’Connor T, Iyer V, Petreanu LT, Hooks BM, Kiritani T, Svoboda K, Shepherd GM. Ephus: multipurpose data acquisition software for neuroscience experiments. Front Neural Circuits. 2010; 4:100. [PubMed: 21960959]

Vastagh C, Gardoni F, Bagetta V, Stanic J, Zianni E, Giampa C, Picconi B, Calabresi P, Di Luca M. N-methyl-D-aspartate (NMDA) receptor composition modulates dendritic spine morphology in striatal medium spiny neurons. J Biol Chem. 2012; 287:18103–18114. [PubMed: 22493505]

Wang H, Stradtman GG 3rd, Wang XJ, Gao WJ. A specialized NMDA receptor function in layer 5 recurrent microcircuitry of the adult rat prefrontal cortex. Proc Natl Acad Sci USA. 2008; 105:16791–16796. [PubMed: 18922773]

Waxman EA, Lynch DR. N-methyl-D-aspartate receptor subtype mediated bidirectional control of p38 mitogen-activated protein kinase. J Biol Chem. 2005; 280:29322–29333. [PubMed: 15967799]

Wei F, Wang GD, Kerchner GA, Kim SJ, Xu HM, Chen ZF, Zhuo M. Genetic enhancement of inflammatory pain by forebrain NR2B overexpression. Nat Neurosci. 2001; 4:164–169. [PubMed: 11175877]

Wei J, Dong M, Xiao C, Jiang F, Castellino FJ, Prorok M, Dai Q. Conantokins and variants derived from cone snail venom inhibit naloxone-induced withdrawal jumping in morphine-dependent mice. Neurosci Lett. 2006; 405:137–141. [PubMed: 16859831]

Weiler N, Wood L, Yu J, Solla SA, Shepherd GM. Top-down laminar organization of the excitatory network in motor cortex. Nat Neurosci. 2008; 11:360–366. [PubMed: 18246064]

Weitlauf C, Honse Y, Auberson YP, Mishina M, Lovinger DM, Winder DG. Activation of NR2A-containing NMDA receptors is not obligatory for NMDA receptor-dependent long-term potentiation. J Neurosci. 2005; 25:8386–8390. [PubMed: 16162920]

Williams AJ, Ling G, Berti R, Moffett JR, Yao C, Lu XM, Dave JR, Tortella FC. Treatment with the snail peptide CGX-1007 reduces DNA damage and alters gene expression of c-fos and bcl-2 following focal ischemic brain injury in rats. Exp Brain Res. 2003; 153:16–26. [PubMed: 12955387]

Xiao C, Huang Y, Dong M, Hu J, Hou S, Castellino FJ, Prorok M, Dai Q. NR2B-selective conantokin peptide inhibitors of the NMDA receptor display enhanced antinociceptive properties compared to non-selective conantokins. Neuropeptides. 2008; 42:601–609. [PubMed: 18992939]

Highlights

- Subunit compositions of NMDARs in L5 pyramidal neurons were focally mapped.
- Spatial expression of NMDARs in pyramidal neurons were assessed in brain slices.
- Selective inhibition of NMDARs in mouse brain was achieved.
- Specific populations of NMDARs can be antagonized in the medial prefrontal cortex.

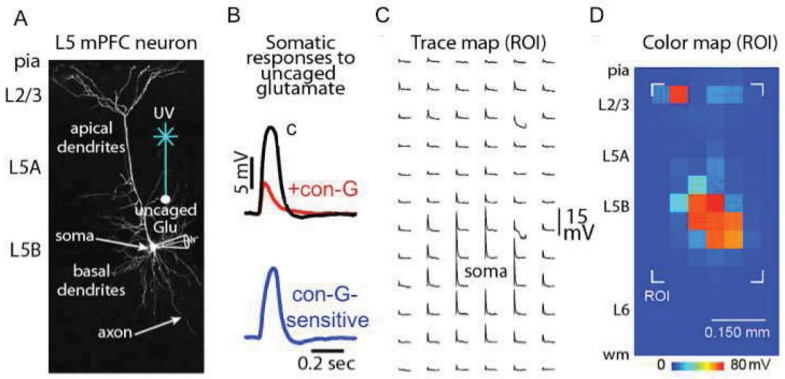

Figure 1.

Analyzing con-G effects on mPFC pyramidal neurons using focal glutamate stimulation. (A) Two-photon image of a layer 5 (L5) neuron in the mPFC depicting the electrophysiology recording configuration from the neuronal soma in combination with focal dendritic stimulation *via* glutamate uncaging. (B, top) Example of excitatory potentials displaying the effects of con-G on the glutamatergic response at a defined dendritic region of the recorded neuron; c = control. (B, bottom) Subtracted trace showing the con-G-sensitive component of the glutamatergic response. (C) Representative trace map showing the spatially-distributed dendritic responses measured at the soma. (D) Corresponding color map showing a ROI (region of interest) which is represented for (C).

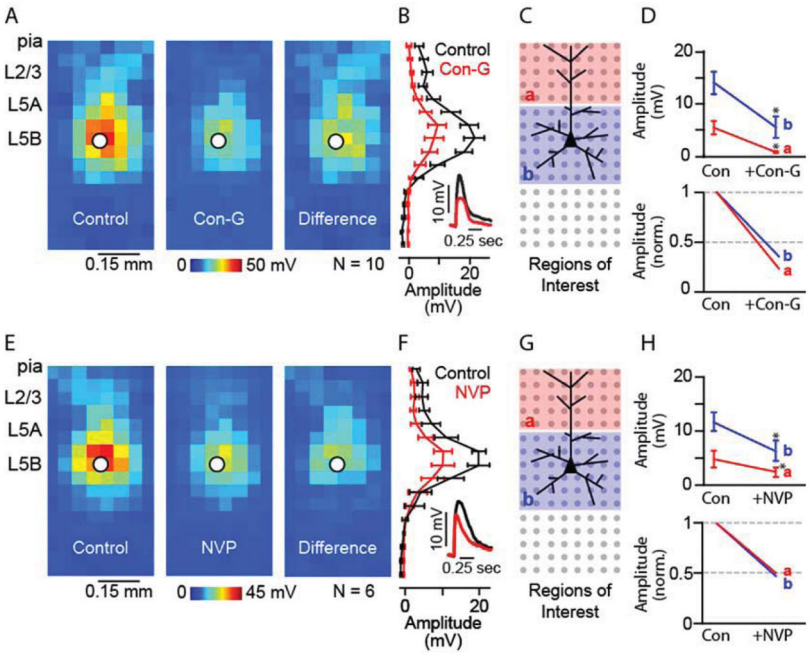

Figure 2.

Con-G and NVP reduce excitatory responses evoked across dendritic arbors by focal glutamate uncaging in L5 pyramidal neurons in the mPFC. (A) Average dendritic map of L5 mPFC neurons before (left) and after (middle) application of con-G. Each pixel represents the mean amplitude of the response evoked by ultraviolet photolysis of MNI-glutamate at that location. Average difference map (right) shows con-G maps subtracted from control maps. (B) Mean (± s.e.m.) vertical profile, calculated by projecting the map of individual neurons to a single vector by averaging along map rows, and then averaging across all neurons. (B, inset) Example response traces before (black) and after (red) application of con-G. (C) Schematic of the stimulation grid (8 × 16; 50 μm spacing), radial orientation of the recorded neuron, and the regions of interest (ROI) for analysis. (D) Absolute (top) and normalized (bottom) magnitude of con-G sensitivity for apical (a) and basal (b) dendrites (*: $p < 0.05$, paired *t*-test), c = control. (E) Average dendritic map of L5 mPFC neurons before (left) and after (middle) application of NVP and the average difference map (right). (F) Mean vertical profile for NVP effects. (F, **inset)** Example response traces before (black) and after (red) application of NVP. (G) ROI schematic. (H) ROI analyses, as in D.

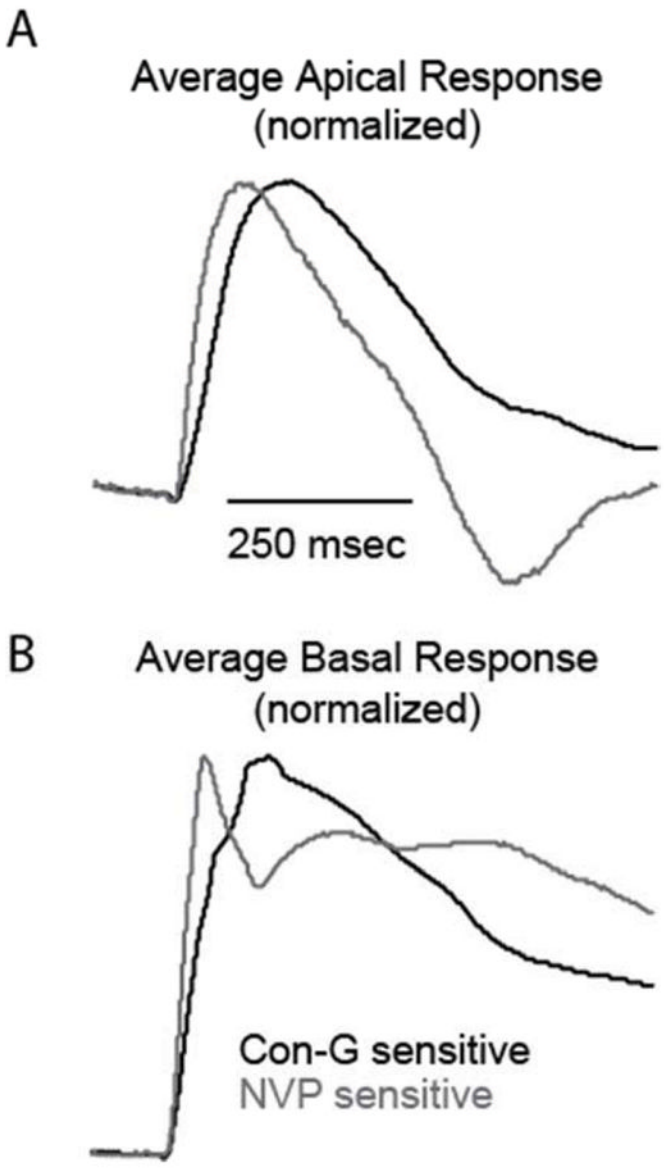

Figure 3.

Con-G and NVP sensitive traces show different kinetics in WT mouse neurons. Average component (normalized to max) of the apical (A) and basal (C) dendritic responses sensitive to con-G and NVP. Traces were generated by subtracting treated from non-treated responses at single apical and basal dendritic locations for each neuron then averaged and normalized.

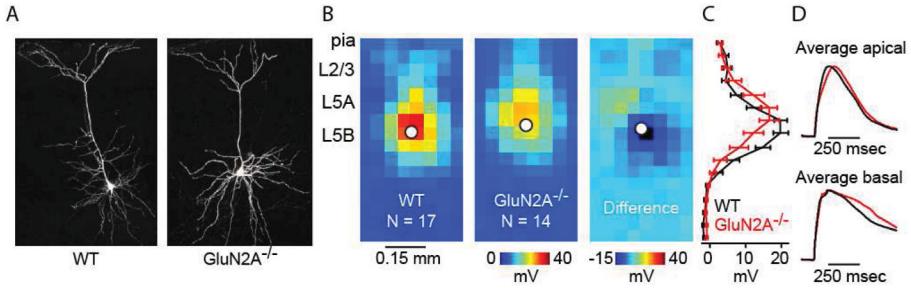

Figure 4.

Glutamatergic responses in GluN2A$^{-/-}$ mice have similar magnitude but different waveforms compared to WT mice. (A) Two-photon images of L5 mPFC neurons in WT and GluN2A$^{-/-}$ mice showing similar dendritic morphology. (B) Average dendritic map of L5 mPFC neurons for WT (left) and GluN2A$^{-/-}$ mice (middle). Average difference map (right) shows GluN2A$^{-/-}$ maps subtracted from WT maps. (C) Mean (± s.e.m.) vertical profile, calculated by projecting a map of each neuron to a single vector by averaging along map rows, and then averaging across all neurons. (D) Average apical (top) and basal (bottom) glutamatergic responses (normalized to the maximum) for WT (black traces) and GluN2A$^{-/-}$ (red traces) neurons.

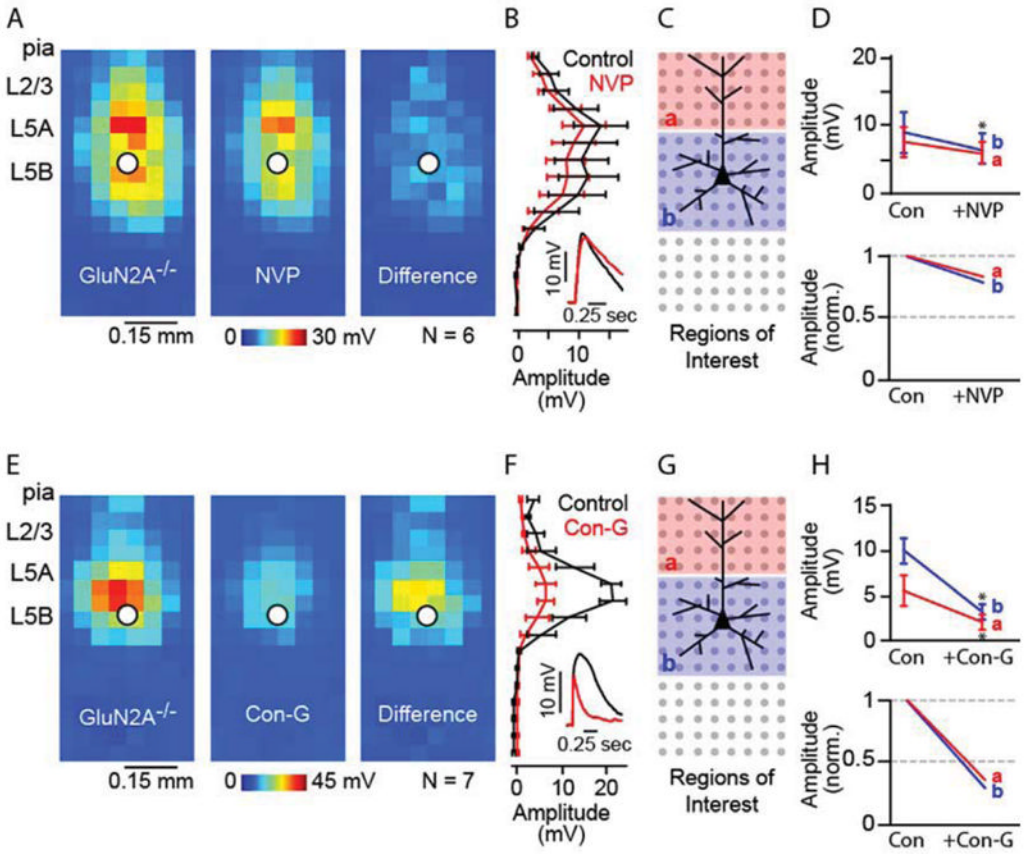

Figure 5.

NVP shows reduced effects on excitatory responses evoked across dendritic arbors in L5 pyramidal neurons in the mPFC of GluN2A$^{-/-}$ mice. (A) Average dendritic map of L5 mPFC neurons before (left) and after (middle) application of NVP. Average difference map (right) shows NVP maps subtracted from control maps. (B) Mean (± S.E.M.) vertical profile, calculated by projecting a map of each neuron to a single vector by averaging along map rows, and then averaging across all neurons. (B, inset) Example response traces before (black) and after (red) application of NVP. (C) Schematic of the stimulation grid (8 × 16; 50 μm spacing), radial orientation of the recorded neuron, and the ROI for analysis. (D) Absolute (top) and normalized (bottom) magnitude of NVP sensitivity for apical (A) and basal (b) dendrites (*: $p < 0.05$, paired *t*-test); c = control. (E) Average dendritic map of L5 mPFC neurons before (left) and after (middle) application of con-G. Average difference map (right) shows con-G maps subtracted from control maps. (F) Mean vertical profile for con-G effects. (F, inset) Example response traces before (black) and after (red) application of con-G. (G) ROI schematic. (H) ROI analyses, as in d.

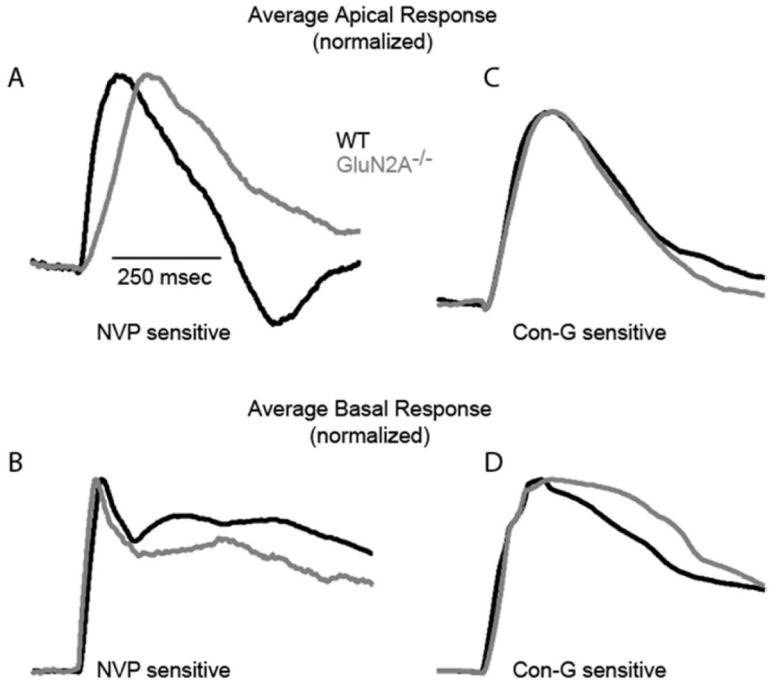

Figure 6.

NVP-sensitive traces show different kinetics between WT and GluN2A$^{-/-}$ mouse neurons. The average component (normalized to max) of the apical (A) and basal (B) dendritic responses sensitive to NVP for WT (black traces) and GluN2A$^{-/-}$ (gray traces) neurons. Average apical (C) and basal (D) dendritic responses sensitive to con-G for WT and GluN2A$^{-/-}$ neurons. Traces were generated by subtracting treated from non-treated responses at single apical and basal dendritic locations for each neuron then averaged and normalized.

Table 1

Effects of Conantokin-G and NVP on gluatmatergic responses

	WT L5 mPFC neurons				GluN2A$^{-/-}$ L5 mPFC neurons			
	Control	**Con-G**	**Control**	**NVP**	**Control**	**Con-G**	**Control**	**NVP**
Apical	4.8±1.0	***1.0±0.2***	4.8±1.4	***2.3 ±0.8***	5.4 ±1.7	***1.8±0.8***	7.5±2.3	5.9±1.7
Basal	13.2±1.6	***5.1±1.5***	11.6±1.5	***6.3±1.9***	9.7±1.4	***2.9± 0.8***	8.8±3.1	***6.4±2.2***

*Bold italics indicate significance; Students paired t-test ($p < 0.05$)

**Values are in millivolts